Received: 17 October, 2011
IOTC-2011-WPTT13-INF12

INFLUENCE OF THE MARINE ENVIRONMENT VARIABILITY ON THE YELLOWFIN TUNA (*THUNNUS ALBACARES*) CATCH RATE BY THE TAIWANESE LONGLINE FISHERY IN THE ARABIAN SEA, WITH SPECIAL REFERENCE TO THE HIGH CATCH IN 2004

Kuo-Wei Lan*, Tom Nishida**, Ming-An Lee*, Hsueh-Jung Lu*, Hsiang-Wen Huang*** , Shui-Kai Chang**** and Yang-Chi Lan*****

Key words: Yellowfin tuna, Arabian Sea, Satellite remote sensing, Principal component analysis.

ABSTRACT

In this study, we collected Taiwanese longline (LL) fishery data and environment variables during the period of 1998–2004 to investigate the relationship between LL catch data of yellowfin tuna (YFT) and oceanic environmental factors using a principal component analysis (PCA).

Results of the PCA showed that monthly variations in catch per unit effort (CPUE) values were significantly correlated with the sea surface temperature (SST), subsurface temperature at 105 m, thermocline depth (horizontal) gradient magnitude, chlorophyll-a concentration, and fish size. April and May were the warmest months of the year in terms of the SST, and the thermocline was generally deep. After July, a drop in the temperature below the preferred temperature range for YFT is probably the reason that the CPUE subsequently decreased in the period of 1998–2003. It was suggested that the CPUE by age at a given time was significantly affected by chlorophyll-a concentrations 1–3 months prior to that time. The lower thermocline depth gradient magnitude enhanced the aggregation density of YFT in 2004 which showed that the high catch and high CPUE of the YFT fishery increased from the western to the eastern Arabian Sea.

I. INTRODUCTION

Yellowfin tuna (YFT; *Thunnus albacares*) is one of the main target species of the commercial tuna longline (LL) fishery and has a long history of being the subject of scientific research in the Indian Ocean. It is a highly migratory and widely distributed species in tropical and subtropical seas of the Pacific, Atlantic, and Indian Oceans, but is absent from the Mediterranean Sea [8]. Taiwan has a long development history in the tuna fishery, and its overall catch of tuna and tuna-like species was ranked as the world's second in recent years [5]. Most of the important tuna catch is made in the Indian Ocean by large-scale LLs [29], and among tuna species, YFT is one of the most important target species in the Arabian Sea and eastern Indian Ocean. Catches of YFT were lower than 20,000 metric tons (mt) before the late 1980s and thereafter substantially increased along with an increase in bigeye-targeting activities utilizing super-cold freezers [11, 23]. However, in this period, the YFT catch increased up to about 80,000 mt in around 1993 and roughly 10 years later was about 40,000–60,000 mt in 2004–2005 [15]. Importantly, most of the Taiwanese catches in these two periods were made in the Arabian Sea [15, 22, 33]. The high catch of the Taiwanese fishery in the Arabian Sea in 2004 implied a notable environmental relationship with the YFT catch rate.

Many studies were conducted on the YFT in the Indian Ocean including the stock structure [35, 42], age determination [12, 42], tropical high-seas resources [13, 14, 35], production models [32], and large-scale oceanographic and long-term average data of YFT distribution patterns [22]. Previous research indicated that the YFT's distribution is mostly concentrated in the Arabian Sea, western tropical waters of the Indian Ocean, and regions around Madagascar [22, 30]. Although the Arabian Sea is an important area for the Taiwanese LL fishery which exclusively targets YFT in the Indian Ocean, the impacts of environmental and oceanographic variables on the fishery are not yet well understood in the Arabian Sea despite the long exploitation history of YFT there.

Biophysical environment factors, such as temperature, salinity, forage (prey), etc., play important roles in controlling the distribution and abundance of tuna [22]. Previous studies indicated that the YFT prefers warm water, and its distribution is affected by the sea surface temperature (SST) [18, 22, 31, 43],

*Department of Environmental Biology and Fisheries Science, National Taiwan Ocean University, 2 Pei-Ning Rd., Keelung 20224, Taiwan, R.O.C.
** National Research Institute of Far Seas Fisheries, Fisheries Research Agency, 5-7-1, Orido, Shimizu-Ward, Shizuoka-City, Shizuoka 424-8633, Japan
***Institute of Marine Affairs and Resource Management, National Taiwan Ocean University, 2 Pei-Ning Rd., Keelung 20224, Taiwan, R.O.C.
****Institute of Marine Affairs, National Sun Yat-sen University, 70 Lienhai Rd., Kaohsiung 80424, Taiwan, R.O.C.
*****Fisheries Research Institute, Council of Agriculture, 199 Hou-Ih Road, Keelung 2024, Taiwan, R.O.C

variations in subsurface sea temperature [2], and the depth of the thermocline [40, 45]. The YFT also occurs in regions with high chlorophyll-a (Chl-a) concentrations and primary productivity [22, 24]. Lee *et al*. [21] suggested that ocean color is a good parameter to express the relationship between the occurrence of fish and potential fishing zones. Remote sensing techniques have great potential to support global fisheries management and the exploitation of pelagic fishes. Joint analyses of satellite and biological/catch data time series can be used to identify changes in pelagic fish habitats and their impacts on migration, size, or recruitment of a particular fish stock, thus helping to regulate maximum catches and preserve fishery resources [52].

The northern Arabian Sea, including the Persian Gulf and Gulf of Oman, is a semi-enclosed sea of the Indian Ocean in Fig. 1. Its biological productivity is influenced by strong physical forcing due to seasonally changing atmospheric conditions [9, 46]. The Arabian Sea is affected by a northeasterly (NE) monsoon from November to February [6, 26, 49]. Strong winds occur again from June to October during the southwesterly (SW) monsoon. During the monsoon seasons, there are complicated circulation patterns consisting of eddies and upwelling.

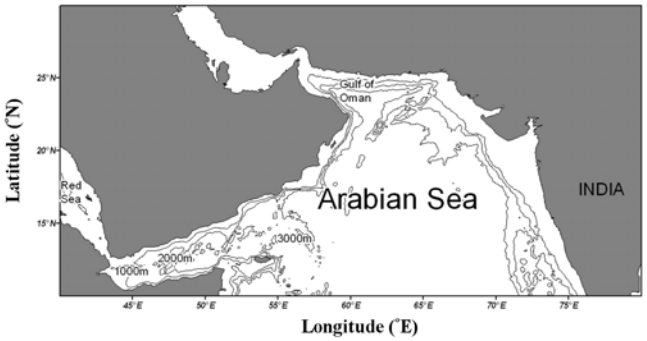

Fig. 1. Map of the study area with bottom topography and geographical names in the Arabian Sea. Land is shaded, and the contours indicate bottom depths in meters.

Satellite imagery depicts a gradient of > 4 °C between the coastal waters of Oman (where upwelling is strongest, and SSTs are usually < 23 °C) and warm water (> 26 °C) of the central Arabian Sea during the SW monsoon season [1, 26]. The northern Arabian Sea is one of the most biologically productive ocean regions in the world. The surface phytoplankton productivity is high off Bombay, Kutch, and Saurashtra (all on India's coast); along Pakistan's coast, and also along the southern part of the Gulf of Oman westward to the south of Yemen [38].

The main goals of this study were to investigate: 1) the spatiotemporal fishing conditions of YFT populations and the distribution associated with variations in oceanographic and biological factors; and 2) the cause of the abnormally high catch in 2004 in the Arabian Sea.

II. MATERIALS AND METHODS

1. YFT fishery data

The catch and effort data were compiled from logbooks of the Taiwanese LL fishery in the Arabian Sea at 10°–30°N and 40°–80°E provided by the Overseas Fisheries Development Council (OFDC) of Taiwan. The catch and effort data were selected from January 1998 to December 2004 to match SeaWiFS Chl-a data. Data included the number of hooks, fishing time, area, catch, and fish size (fork length in cm) of the YFT and were geographically referenced and averaged to obtain monthly means on a 5° x 5° spatial grid.

2. Environmental data

We used three kinds of satellite-derived and model-simulated data in this study: (1) Chl-a, (2) SST, and (3) model-simulated sea temperatures at depths of 5–459 m. We used Global Area Coverage (GAC) monthly composite SeaWiFS images downloaded from the NASA Ocean Color Web with a 9-km spatial resolution from January 1998 to December 2004. The ocean colors of SeaWiFS level 3-mapped images were used to estimate the sea surface Chl-a. Satellite-derived SST data were collected from the Advanced Very High Resolution Radiometer (AVHRR) on board the National Oceanic and Atmospheric Administration (NOAA) satellites and downloaded from the National Environmental Satellite, Data, and Information Service (NESDIS). The AVHRR SST data with a spatial resolution of 4 km were processed through the Multichannel Sea Surface Temperature (MCSST) algorithm vers. 4 [25] at a ground station of National Ocean Taiwan University [20]. In addition, subsurface temperature data were produced by the National Center for Environmental Prediction model (NCEP) into vertical profiles with data every 10 m from 5 to 459 m in depth with a 1/2° × 1/3° spatial resolution. The NCEP model is driven by the global atmospheric heat and momentum fluxes produced four times daily at the NCEP. Chl-a, SST, and subsurface temperature data were then calculated as monthly means on a spatial grid of 5° x 5° from January 1998 to December 2004. The 5° x 5° grid environmental data used in this study matched the resolution of the fisheries data.

3. Data analysis

The depth of the 20 °C isotherm was calculated and assumed to be the thermocline depth (TD_20), which is a good indicator of the seasonal-to-interannual variability in the thermocline in the study area [51]. In order to comprehend spatial and temporal variations in the TD_20 in different areas, the thermocline depth (horizontal) gradient magnitude (TDGM) was further calculated to investigate the 2-dimensional variability of the thermocline. The TDGM was computed at the above-specified depths across the thermocline in the Arabian Sea by the following equation:

$$\mathrm{TDGM} = \sqrt{(\partial \mathrm{D}/\partial x)^2 + (\partial \mathrm{D}/\partial y)^2} \quad ; \quad (1)$$

where D is thermocline depth in 5° x 5° cells in the Arabian Sea, and the x- and y-axes are longitude and latitude, respec-

tively. The TDGM was computed for each 5° x 5° cell for each month. The TDGM portrays 2-dimensional variability of the thermocline depth, which is an indicator of the spatial variability of deep water in the Arabian Sea. The TDGM composite map reveals dynamic features of the Arabian Sea thermocline. The Taiwanese LL fishery primarily targets YFT at an operational depth of 50–120 m in the Indian Ocean [23] where temperatures are generally > 20 °C, and the YFT is abundant [3]. This study used subsurface temperatures in the layer of 55–125 m in the cross-correlation analysis to eliminate spurious high correlation factors [47] (Tsai and Chai, 1992). The subsurface temperature at 105 m (ST_105) was then chosen as an indicator of the subsurface temperature variation factor. Chl-a and Chl-a 1-3 months (Chl-a_D1–Chl-a_D3) prior to the present catch per unit effort (CPUE) were selected to investigate the lag effect of trophic transformation of YFT's forage material [19]. All environmental factors used in this study are summarized in

Table 1. Environmental factors selected from satellite-derived and model assimilation data in this study

Variable	Category	Annotation
Temperature	SST	Sea surface temperature
	ST_105	Temperature at 105 m in depth
Chlorophyll-a (Ocean color)	Chl-a	Mean value of chlorophyll-a
	Chl-a_D1	Mean value of chlorophyll-a 1–3 months prior to the present catch rates
	Chl-a_D2	
	Chl-a_D3	
Thermocline depth	TD_20	Depth at 20 °C
Thermocline depth gradient magnitude	TDGM	Two-dimensional variability in the change in the thermocline

Table 1.

The CPUE consisted of the catch rate (number) per month and used as a relative abundance index of the YFT. It was calculated as the number of individuals captured by 1000 hooks (individuals (ind.)/10^3 hooks) on a spatial grid of 5° x 5°, and values were integrated into monthly averages. For the age and growth of the YFT in the Arabian Sea, the method of [42] was used to identify different fish sizes (cm) of the YFT in four groups as shown in Table 2: size group A (age ≤ 2.5 yr, (length ≤ 105 cm)); size group B (aged > 2.5, (length > 105 cm) and ≤ 3 yr (≤ 119.2 cm)); size group C (aged > 3 yr (length > 119.2 cm) and ≤ 3.5 yr (length ≤ 132.2 cm)); and size group D (aged > 3.5 yr (length > 132.2 cm)).

Before the principal component analysis (PCA), standardization of the nominal CPUE of YFT was carried out using a generalized linear model (GLM) to remove the effect of factors that may bias the CPUE as an index of abundance [28] and lead to artificial overestimation [50]. The main factors considered in this analysis were year, month, area, and numbers of hooks between two floating balls (NHB), and interactions between the main factors were also included in the model:

$$\log(CPUE+c) = \mu + YY + MM + Area + NHB + Interactions + \varepsilon; \quad (2)$$

where CPUE is the nominal CPUE of YFT, c is the 10% of overall mean of the CPUE,μ is the intercept, YY is the effect of year (1998–2004), MM is the effect of month (January–December), Area is the effect of fishing area (14 areas), NHB is the number of hooks between two floating balls (6-20 hooks), Interactions is the interactions between the main factors, and ε is an error term.

The Akaike Information Criterion (AIC) was used to select among alternative models, and the one with the lowest value of the AIC was selected as the "best" model. The standardized

Table 2. Age and growth used to estimate different fish sizes (cm) of the YFT in four groups in the Arabian Sea

Group	A	B	C	D
Age (yr)	≤ 2.5	> 2.5 and ≤ 3	> 3 and ≤ 3.5	> 3.5
Length (cm)	≤ 105	> 105 and ≤ 119.2	> 119.2 and ≤ 132.2	> 132.2

CPUE was then computed from the adjusted means (least square means) of the estimates of the interaction term between year and month effects. The ANOVA tables for the selected model are shown in Table 3.

We examined five environmental variables: SST, ST_105, TD_20, TDGM, and Chl-a measured by multiple satellite and model simulations. Thirteen factors including fishery data (CPUE and fork length (cm) of each level) and oceanic environmental factors were chosen for the PCA. Data were standardized using the formula described by Johnson and Wichern [16] for the PCA. The principal component can be standardized by a correlation matrix instead of a covariance matrix if the units of the factors differ [10, 41]. Both Fung and LeDrew [10] and Eastman and Fulk [7] indicated that a standardized PCA has a better alignment along the object of interest and appears to be more effective than an unstandardized PCA for detecting changes. Monthly fishery data and environmental variables were used as independent variables. Data of each variable were standardized by a linear transformation using the formula:

$$\frac{X_i - \overline{X}}{S.D.}; \quad (3)$$

where Xi is the datum of month i, and $\overline{X}$ and S.D. are the relative mean and standard deviation of the data, respectively [16]. A factor analysis model of the PCA was used to describe associations of the YFT with environmental variations. Eigenvalues and proportions of dependent and independent variables were selected according to factor loading and cumulative proportions of the variables. The principal component scores were estimated by the following formula:

$$Z_i = \sum_{j=1}^{n} E_{ij} \times S_{ij}; \quad (4)$$

where Zi is the score of principal component i; Eij is the eigenvalue of variable j of principal component i; and Sij is the standardized value of variable j of principal component i. A principal component with a high proportional value suggests that it has a better distribution and thus better relationships among its elements. A geographical information system (GIS) was used to construct a database of the fishery and environmental datasets. Statistical analyses were performed using

StatSoft Statistica 6.0.

III. RESULTS

1. Temporal variations in environmental factors and the CPUE

Table 3 shows the ANOVA table for the selected model and R^2 values explained about 58% of the variance. Time series of the nominal and standardized CPUEs of YFT in 1998-2004 are shown in Fig. 2, and the standardized CPUE roughly followed the pattern of the nominal CPUE. The time series of nominal and standardized CPUEs (1998–2004) showed that the major fishing season in the Arabian Sea is from the first (January–March) to second (April–June) quarters (Fig. 2), and the highest values occurred in the second quarter, with a standardized CPUE of about 3.67–20.20 ind./10^3 hooks. Quarterly catches of the YFT varied 158.3–5476.6 mt in the first and second quarters from 1998 to 2003 (Fig. 2a, b). In 2004, the monthly catch was double those of other years, having increased from 1302.4 mt in the first quarter to 11,126.5 mt in the second quarter. During the fishing season (January-June), averages of environmental factors varied: SST ranged 25.1–29.3 °C (Fig. 3a), ST_105 ranged 21.7–23.4 °C (Fig. 3b), TD_20 ranged 100.8–141.9 m (Fig. 3c), and Chl-a ranged 0.38–0.66 mg/m3 (Fig. 3d). The CPUE and catch appeared to be lower in the third quarter (July–September) with relatively lower SST, lower ST_105, shallower TD_20, and higher Chl-a values. In the fourth quarter (October–December), SST rose to 28.2 °C in October, but ST_105 continued to fall from October to December (< 21.7 °C).

Table 3. ANOVA table for the selected model of the generalized linear model

Source	df	SS	MS	*F*-value	*p* value	R^2
Model	146.00	4237.36	29.02	66.75	< 0.001	0.58
Error	6726.00	2924.40	0.43			
Corrected total	6872.00	7161.76				

Source	df	SS	MS	*F*-value	*p* value
YY	6	53.28	8.88	20.43	< 0.001
MM	11	37.75	3.43	7.89	< 0.001
Area	12	74.92	6.24	14.36	< 0.001
NHB	1	4.50	4.50	10.35	< 0.001
YY * MM	27	477.01	17.67	40.63	< 0.001
YY * Area	34	183.73	5.40	12.43	< 0.001
MM * Area	49	351.69	7.18	16.51	< 0.001

df, degrees of freedom; SS, sum of squares; MS, mean square; YY, the effect of year; MM, the effect of month; Area, the effect of fishing area; NHB, the number of hooks between two floating ball

2. Spatial distribution of the CPUE

Because a high catch occurred in 2004, data of the nominal CPUE spatial distribution were divided into two periods, 1998–2003 and 2004 (Figs. 4, 5), for further comparisons. The YFT aggregates in the Arabian Sea at 10°–25°N and 52°–72°E (Fig. 4), and the major fishing period for YFT begins in the first quarter and ends in the third quarter. The monthly means of nominal CPUE in 1998–2003 indicated that areas of CPUE of > 10 ind./10^3 hooks were concentrated in the western Arabian Sea at 10°–25°N and 55°–65°E in the second quarter. On the other hand, areas of nominal CPUE of < 10 ind./10^3 hooks were mainly in the eastern Arabian Sea south of 15°N. In 2004, spatial distributions in the Arabian Sea differed. Areas with a high nominal CPUE (of > 10 ind./10^3 hooks) in the first quarter appeared on the northeastern side (15°–25°N and 55°–70°E) (Fig. 5) where nominal CPUE values had been lower in 1998–2003.

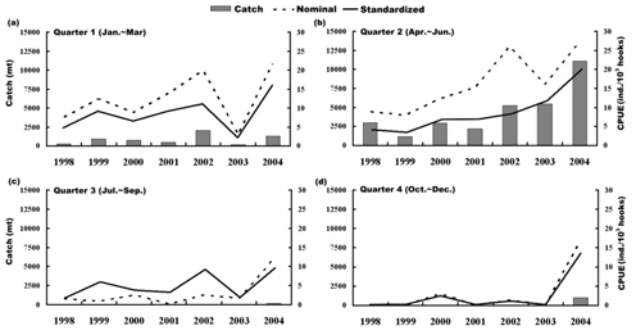

Fig. 2. Quarterly trends of nominal (black dotted line) catch per unit effort (CPUE) and standardized CPUE (black line) and catch (gray bar chart) of yellowfin tuna caught by the Taiwanese longline fishery in the (a) first quarter (January–March) (b) second quarter (April–June) (c) third quarter (July–September) and (d) fourth quarter (October–December) in 1998–2004.

3. PCA analysis of the CPUE and environmental indices

The standardized CPUE and fork length (cm) of each level in relation to environmental factors in the major fishing period (January to June) were predicted by the PCA. The percentage variance and eigenvalue of each principal component are given in Table 4. Three principal components had eigenvalues of > 1. We decided to use the corresponding first (42.09%), second

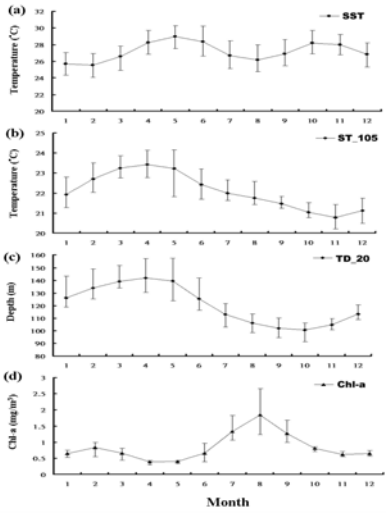

Fig. 3. Temporal variability in (a) sea surface temperature, (b) sea temperature at 105 m, (c) thermocline depth (the depth of the 20 °C isotherm), and (d) chlorophyll-a in 1998–2004.

(16.33%), and third eigenvalues (13.29%) which accounted for 71.71% of the cumulative variance.

Factor loadings of the first three components of the PCA of 13 variables are listed in Table 5. Factor loadings of highly positive correlations with CPUE (-0.63) for the first component were SST (-0.64), ST_105 (-0.86), TD_20 (-0.82), Chl_D2 (-0.61), Chl_D3 (-0.73), and size groups C (-0.60) and D (-0.70); and those with highly negative correlations were TDGM (0.78) and Chl-a (0.91). The second component represents highly positive correlations with Chl-D1 (-0.59), Chl-D2 (-0.57), and size group A (-0.56), and the first component also represents highly positive correlations with Chl-D2, Chl-D3, and size groups B and D. These relationships suggest that a 1–3-month lag of Chl-a may influence the activity of different-aged tuna schools because of the availability of foraging material. The third component showed highly positive correlations with CPUE (-0.54) and size group B (-0.65). Scatterplots of the first and second component axes in Figs. 6 and 7 illustrate the distribution patterns of environmental factors associated with fishery factors and monthly variations, respectively. The associations indicate that the CPUE increased with higher sea temperatures, a deeper thermocline, and lower Chl-a values in April and May, but then the CPUE decreased in June at the beginning of the summer monsoon season due to lower sea temperatures and higher Chl-a levels. The PCA results also imply that an increase in the proportion of size group B YFT (third component) and a decrease in the TDGM (first component) in the Arabian Sea resulted in a high CPUE.

Table 4. Eigenvalues and the variance cumulative percentage for the principal component analysis

Principle component	Eigenvalue	Variance (%)	Cumulative variance (%)
1	5.47	42.09	42.09
2	2.12	16.33	58.42
3	1.73	13.29	71.71
4	0.94	7.25	78.96
5	0.82	6.33	85.29
6	0.52	4.02	89.32
7	0.38	2.93	92.25
8	0.32	2.48	94.72
9	0.26	2.03	96.75
10	0.15	1.16	97.91
11	0.11	0.88	98.79
12	0.10	0.79	99.59
13	0.05	0.41	100.00

Table 5. Results of the principal component analysis from the first (PC1) to the third principal component (PC3) for environmental factors with yellowfin tuna standardized catch per unit effort (CPUE) and four categories of body length (cm)

	Principal component		
Variable	PC1	PC2	PC3
SST	-0.64	0.43	-0.43
ST_105	-0.86	0.09	0.34
TD_20	-0.82	0.29	0.34
TDGM	0.78	0.15	-0.36
Chl-a	0.91	-0.06	0.07
Chl_D1	0.31	-0.59	0.56
Chl_D2	-0.61	-0.57	0.27
Chl_D3	-0.73	-0.40	-0.20
CPUE	-0.63	-0.45	-0.54
Size group A	-0.33	-0.56	0.08
Size group B	-0.27	-0.40	-0.65
Size group C	-0.60	0.24	-0.10
Size group D	-0.70	0.45	0.14

SST, sea surface temperature; ST_105, temperature at 105 m; TD_20, the depth at 20 °C; TDGM, thermocline depth gradient magnitude; Chl-a, mean value of chlorophyll-a; Chl-a_D1-D3, mean value of chlorophyll-a 1–3 months prior to the present catch rates; Size groups A–D, fish sizes (cm) of the YFT

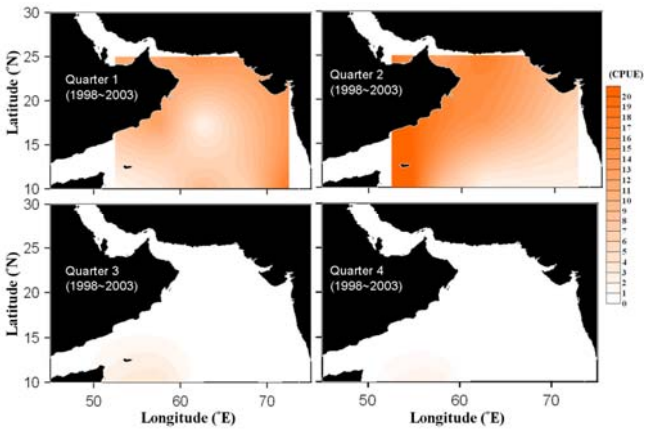

Fig. 4. Nominal catch per unit effort (CPUE) distributions pattern of yellowfin tuna for four quarters in the Arabian Sea (mean value of 1998–2003 Taiwanese longline fishery data of a 5° x 5° grid). The white region indicates no fishery data in those areas.

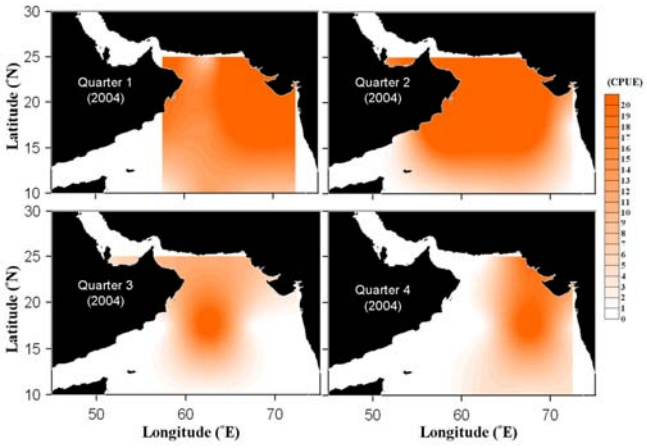

Fig. 5. Nominal catch per unit effort (CPUE) distributions pattern of yellowfin tuna for four quarters in the Arabian Sea (mean value of 2004 Taiwanese longline fishery data of 5° x 5° grid). The white region indicates no fishery data in those areas.

4. Temporal and spatial variations in the TDGM

The TDGM showed a highly negative eigenvalue with the standardized CPUE in the first principal component. This implies that a lower TDGM in the Arabian Sea would cause a high CPUE. Figure 8 shows temporal and spatial variations in the TDGM in the Arabian Sea at 50°–70°E and 15°–20°N during the fishing seasons from 1998 to 2004. High values in Fig. 8 (in yellow and red) indicate higher gradient magnitudes of the

thermocline, and low values (in green and blue) reveal lower gradient magnitudes. Figure 8 depicts that from February to July (1998–2003), the thermocline depth was usually lower (gradient magnitude 3–30 m/5°, blue color) in the western and central parts (55°–65°E) than on the eastern side (65°–70°E) (gradient magnitude 30–54 m/5°). In June and July, the gradient magnitudes on the western side increased from 30 to 45 m/5°, and a similar rise also occurred in the east. Variations in the TDGM differed in 2004. The lower TDGM of 6–24 m/5° extended from the western to the eastern Arabian Sea from February to July. This implies that the thermocline depth was shallow and had similar gradient magnitudes from west to east in the Arabian Sea in March–July 2004. A high CPUE usually occurred in the western Arabian Sea (Fig. 4) with a gradual change in the thermocline depth (i.e., a lower TDGM in Fig. 8). In 2004, the TDGM (6–24 m/5°) on the eastern side from March to July was lower than in other years with a high nominal CPUE. Unlike the long-time pattern of the average nominal CPUE, the shallow thermocline depth (lower TDGM) occurred on the eastern side in 2004 enhancing aggregation of

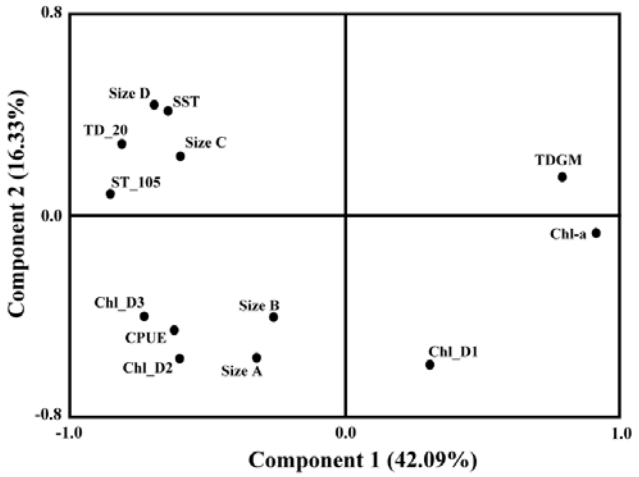

Fig. 6. Ordination diagram of the principal component analysis (first and second principal components) showing the indicator catch per unit effort (CPUE) and four categories of body length in relation to environmental factors in the four quadrants. Black circles indicate vectors of each factor in the quadrants.

YFT density, as the CPUE of YFT increased from the western to the eastern Arabian Sea.

IV. DISCUSSION

Seasonal variations in hydrographic conditions can be broadly and immediately observed by satellite remote sensing [20]. Understanding the effects of environmental conditions on fish populations is an essential step toward ecosystem-based management of fisheries, which is increasingly becoming a standard approach in management policies [37]. In the Arabian Sea, the major period for catching YFT begins in the first quarter and ends in the third quarter, and the CPUE of YFT also shows seasonal changes. Stretta [43] indicated that in the tropics, most YFT prefer warm water with a narrow temperature range of 22–29 °C, particularly above 25 °C. In the Indian Ocean, YFT are distributed in regions where SSTs are > 25 °C [18, 22], which was confirmed by the present study. In the Arabian Sea, April and May, with the highest CPUE, were the warmer months of the year with an average SST range of 28.3–29.0 °C (Fig. 3a). The SST began to decrease in July and

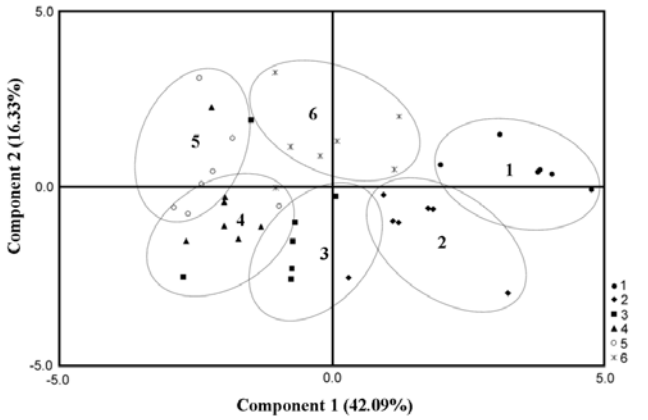

Fig. 7. Ordination diagram of the principal component analysis (first and second principal components) showing the monthly evolution in the Arabian Sea (numbers 2 to 7, sites of the mean scores of respective months from February to July).

reached the lowest SST of 26.1 °C in August.

In our PCA results, the first principal component showed that SST was not the only major environmental factor, as ST_105 and TD_20 revealed higher positive correlations with the standardized CPUE than did SST. This suggests a higher ST_105 led to a deeper thermocline depth and, therefore, a higher catch of YFT. The Taiwanese LL fishery targeting YFT has an operating depth of 50–120 m in the Indian Ocean [23], where temperatures generally exceed 20 °C, and the YFT is abundant. In the Arabian Sea, values of ST_105 in February–June were more suitable for YFT, but the descending temperature from July went beyond the preferred temperature range for YFT. With regard to the decreases in SST and ST_105 after July in the Arabia Sea, Rixen *et al*. [39] interpreted that they were due to the cool, steady, and strong SW monsoon in summer, which generated extensive coastal upwelling and eddy advection over the margin of the continent in the NW Indian Ocean. Nutrients injected into the Arabian Sea from cold upwelling water support higher rates of primary productivity (> 2.5 mg C m^{-2} d^{-1}) than found in the area outside of the upwelling, at about 1 mg C m^{-2} d^{-1} [1, 4]. This also illustrates that Chl-a is highly negatively related to the CPUE in the first principal component. The temperature at the top of the thermocline was always > 20 °C where the YFT catch by the LL fishery was high [40, 45]. In the eastern tropical Pacific, a sharp oxycline accompanying the thermocline further tends to limit the depth range of YFT [44]. In this study, we also found that the CPUE of YFT varied with the depth of the TD_20; we thus suggest that ST_105 and TD_20 are good indicators of seasonal-to-interannual variability of the CPUE of YFT in the Arabian Sea.

The PCA results showing that Chl-a 1–3 months prior to the present CPUE possibly influenced catch rates and different-aged tuna schools were probably due to a lag effect of trophic transformation. This is similar to a report by Ortega-Garcia and Lluch-Cota [36] which found a positive relationship of high tuna abundance with a 3–5-month delay in high pigment concentrations in the tropical Pacific. In the Arabian Sea, surface phytoplankton production generally increases in winter [27], and high Chl-a values were exclusively concentrated along the southern part of the Gulf of Oman. Tang *et al*. [46] suggested that the impact of wind stress of the NE monsoon on upwelling of the northern Arabian Sea brings nutrient-rich subsurface water to the surface and results in phytoplankton blooms in the area. Steep bathymetric areas, such as continental slopes, sea mounts, and sea canyons, often produce upwelling, which forces nutrient-rich waters to the surface, thereby forming good tuna fishing grounds [33]. Figure 4 shows that high nominal CPUE areas were always concentrated in the western Arabian Sea close to the Gulf of Oman where Chl-a values were high [27, 46]. Kaymaram [17] noted that fishing grounds and fishing periods in the Gulf of Oman are well known to be associated with upwelling and high productivity. The time lag of Chl-a related to the CPUE suggests that the forage concentration is an attractive factor which

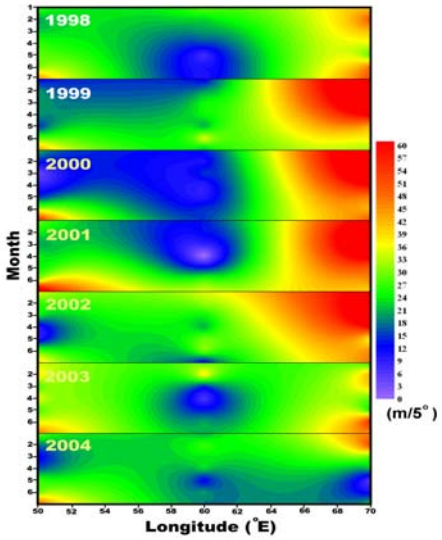

Fig. 8. Temporal and spatial variations in the thermocline depth gradient magnitude in the Arabian Sea (15°–20°N and 50°–70°E) in 1998–2004.

causes aggregation of different-aged tuna schools, and consequently influences spatial distribution patterns of the YFT.

Explaining the high catch and high CPUE of YFT in 2004 is also one of the important parts of our research. The reasons for the high catch and high CPUE in 2004 differed from those in 1993. Figure 9 shows quarterly trends of the nominal CPUE, *i.e*., the catch and effort of the Taiwanese LL fishery in 1991–2004. Although the catch was highest in the second quarter of 1993, the effort was also highest among these 14 years. Nishida *et al*. [33] indicated that very few LL vessels fished in the Arabian Sea before 1993, and many Taiwan LL vessels suddenly began to enter that area as a virgin fishing ground once good fishing conditions were found. Thus, in addition to the good fishing conditions, expanded fishing effort by many LLs is also one of the causes for the high YFT catch in 1993. But the high catch and high CPUE were likely mainly caused by large ecological anomalies in 2004. Usually, a high CPUE occurs in the western Arabian Sea (Fig. 4) with a gradual

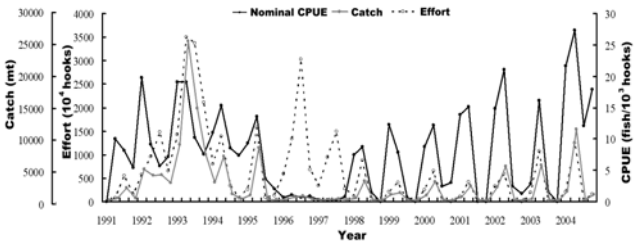

Fig. 9. Quarterly trends of nominal catch per unit effort (CPUE; black line), catch (gray line) of yellowfin tuna, and effort (black dotted line) of the Taiwanese longline fishery in 1991–2004.

change in the thermocline depth (i.e., a lower TDGM in Fig. 8). Variations in the thermocline depth in 2004 differed from those of other years. In 2004, the TDGM (6–24 m/5°) on the eastern side from March to July was shallower than that in other years. The shallow thermocline depth on the eastern side resulted in a close similarity of gradient magnitudes throughout the Arabian

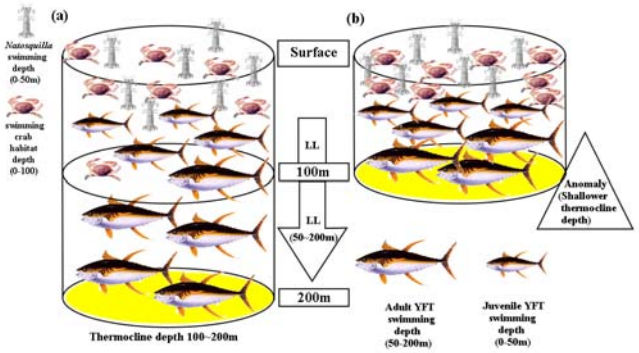

Fig. 10. Aggregation of yellowfin tuna and its prey (Natosquilla and swimming crabs) in shallower waters due to a shallower thermocline depth: (A) the general situation (1998–2003) and (B) the situation in 2003–2004. Redrawn from Nishida *et al*. (2005).

Sea. Unlike the long-time pattern of the average nominal CPUE, areas of high nominal CPUE were also concentrated on the northeastern side of the Gulf of Oman (Fig. 5), and a shallow thermocline depth (a lower TDGM) occurred on the eastern side, which enhanced aggregation density, as the high CPUE of YFT increased from the western to the eastern Arabian Sea. Nishida *et al*. [32] also indicated that in 2003–2004, there were negative anomalies of SSTs and subsurface temperatures in the Arabian Sea, so the layer of water where the YFT usually inhabited became cooler than normal (Fig. 10), and the thermocline depth was much shallower. Adult YFT usually stay at 50–200 m above the thermocline, but during 2004 they were likely to have moved to much-shallower waters as the thermocline depth became shallower. Sund *et al*. [44] indicated that an

elevated thermocline may lead YFT to concentrate near the surface. We therefore speculated that the occasionally shallower thermocline in the entire Arabian Sea may have forced the YFT to move to upper waters. As a consequence, YFT aggregated in highly dense schools due to the west-to-east extension of shallower thermocline depths, thus increasing the

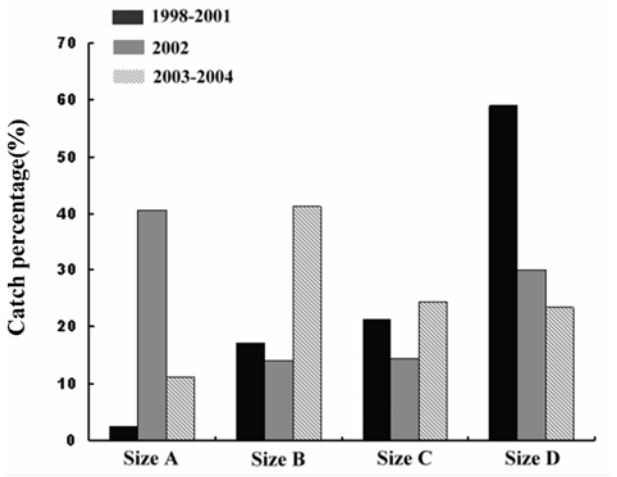

Fig. 11. Catch percentage of four categories of body length (size group A–D): black bar, average of 1998–2001; gray bar, 2002; lined bar, average of 2003 and 2004.

catch probability in 2004.

Another reason for the high catch and high CPUE of YFT may have been recruits. The third principal component indicates a high positive eigenvalue of the standardized CPUE and size group B. In other words, increasing the proportion of size group B YFT may have resulted in a high CPUE. Nishida *et al*. [32] indicated that the high catch of YFT in 1993 was probably caused by strong recruitment in 1991 in the Arabian Sea, because of favorable environmental conditions such as strong upwelling for spawners in the spawning areas near Oman. It was speculated that YFT in the Gulf of Oman are highly migratory when feeding and spawning within this area, and then they move into more-southerly waters. Before 2002, the length of YFT caught in the Arabian Sea mostly belonged to size group D (60%), which is over the age of 3.5 years (Fig. 11). But in 2002, over 40% of the YFT were smaller than the size at 2.5 years old (size group A). The high recruitment of size group A in 2002 consequently caused the large YFT population of size group B (> 40%) in 2003–2004. Therefore we suggest that the high catch of YFT in 2004 may have been due to high recruitment in 2002. Nishida *et al*. [33] stated that the Japanese LL fishery had a high catch of YFT in 2003 in the western tropical Indian Ocean, likely because of substantial ecological anomalies such as abnormally strong upwelling which enhanced strong food web reactions from primary producers, plankton, and prey for YFT causing aggregation of YFT. In this study, we also found that a change in the TDGM and the influence of recruitment in 2003 were not as apparent as in 2004 in the Arabian Sea.

The availability of biological and oceanographic information would obviously help fishery operations and would lead to better management of these resources. A better understanding of relationships between oceanic environments and fishing conditions could make utilization of YFT more efficient, profitable, and sustainable. But it is hard to explain how particular changes in the thermocline depth are related to the environment in our analysis. Rather, we identified several issues for future research. First, there is a need to collect more long-term LL data from different countries and expand the area of investigation beyond the Arabian Sea to the western Indian Ocean. Second, the prey of YFT such as cephalopods and small pelagic fish and the relationship of their abundance to primary production also need to be examined. Third, effects of the monsoon and oceanic currents on changes in the thermocline depth in the area need to be analyzed in the future.

V. CONCLUSIONS

1. The major fishing season in the Arabian Sea begins in the first quarter and runs to the third quarter, with the highest value (CPUE and amount of catch) occurring in the second quarter. In the second quarter, the SST is the warmest of the year with a deep thermocline depth. After the second quarter, the temperature drops out of the preferred temperature range for the YFT, probably resulting in a lowering of the CPUE which is lower from July to December.

2. High-CPUE areas are always concentrated in the northern Arabian Sea close to the Gulf of Oman where Chl-a values are high. A significant time lag of standardized CPUE and different sizes (cm) of YFT related to Chl-a with a time lag of 1–3 months suggest that the occurrence of foraging materials influences the congregation of YFT schools.

3. The lower TDGM with a shallow thermocline depth enhancing the aggregation density of YFT shows that the CPUE of YFT increased from the western to the eastern Arabian Sea, and subsequently a high catch occurred in 2004.

4. In 2004, the standardized CPUE was also significantly related to the occurrence rate of a YFT length of 105–120 cm, suggesting that the high catch in 2004 was associated with higher recruitment in 2002.

VI. ACKNOWLEDGEMENTS

This study was financially supported by the Council of Agriculture (95AS-14.1.2-FA-F2 and 97AS-15.1.2-FA-F3) and National Science Council (NSC95-2611-M-019-016), Taiwan. We are grateful to the Overseas Fisheries Development Council (OFDC) of Taiwan for providing data from the Taiwanese longline fishery and the National Research Institute of Far Seas Fisheries, Fisheries Research Agency of Japan for the model-simulated subsurface temperature data. Professor C.T. Shih of National Taiwan Ocean University, Keelung, Taiwan and Prof. I.M. Belkin of the University of Rhode Island, RI, USA kindly helped revise the grammar of the manuscript. Finally, we would like to express our appreciation to Ms. Jui-wen Chan and Wei-Jiuan Shieh for their assistance in extracting sea surface temperature and chlorophyll-a images.

REFERENCES

1. Anderson, D. M., Brock, J. C., and Prell, W. L., "Physical upwelling processes, upper ocean environment and the sediment record of the southwest monsoon," *Geological Society, London, Special Publications,* Vol. 64, pp. 121-129 (1992).
2. Bautista-Cortes, L. F., *Análisis de la pesquería Mexicana de atún, con énfasis en tres tipos de indicadores de cardúmenes. Tesis de Maestría en Ciencias*, CICIMAR. Instituto Politécnico Nacional, México, 69 pp (1997).
3. Blackburn, M., "Oceanography and the ecology of tunas," *Oceanography and Marine Biology: An Annual Review*, Vol. 3, pp. 299-322 (1965).
4. Brock, J.C., McClain, C. R., Anderson, D. M., Prell, W. L., and Hay, W. W., "Southwest monsoon circulation and environments of recent planktonic Foraminifera in the northwestern Arabian Sea," *Paleoceanography*, Vol. 7, No. 6, pp. 799-813 (1992).
5. Chang, S. K., Liu, K. Y., and Song, Y. H., "Distant water fisheries development and vessel monitoring system implementation in Taiwan-History and driving forces," *Marine Policy*, Vol. 34, No. 3, pp. 541-548 (2010).
6. Dennett, M. R., Caron, D. A., Murzov, S. A., Polikarpov, I. G., Gavrilova, N. A., Georgieva, L. A., and Kuzmenko, L.V., "Abundance and biomass of nano- and microplankton during the 1995 northeast monsoon and spring intermonsoon in the Arabian Sea," *Deep Sea Research Part II*, Vol. 46, pp. 1691-1717 (1999).
7. Eastman, J. R., and Fulk, M., "Long sequence time series evaluation using standardized principle components," *Photogrammetric Engineering and Remote Sensing*, Vol. 59, pp. 991-996 (1993).
8. FAO Fisheries Department, World review of highly migratory species and straddling stocks," *FAO Fisheries Technical Papers*, Vol. 337, pp. 1-70 (1994).
9. Findlater, J., "A major low-level air current near the Indian Ocean during the northern summer," *Quarterly Journal of the Royal Meteorological Society*, Vol. 95, No. 404, pp. 362-380 (1969).
10. Fung, T., and LeDrew, E., "Application of principal components analysis change detection," *Photogrammetric Engineering and Remote Sensing*, Vol. 53, pp.1649- 1658 (1987).
11. Hsu, C. C., Lee H. H., Yeh Y. M., and Liu H. C., "On targeting problem, partitioning fishing effort and estimating abundance index of bigeye tuna for Taiwanese longline fishery in the Indian Ocean, " *IOTC Proceedings*, Vol. 4, pp. 279-292 (2001).
12. Huang, C. C., Sun, L., and Yang R. T., "Age, growth and population structure of the Indian yellowfin tuna," *Journal of the Fisheries Society of Taiwan*, Vol. 2, No. 1, pp. 16-30 (1973).
13. IOTC, "Report on the status of the databases held at the IOTC secretariat," *IOTC Proceedings*, Vol. 4, pp. 256-265 (2001).
14. IOTC, "Status of IOTC databases for tropical tunas," *IOTC Secretariat*, Vol. 1, pp. 1-25 (2004).
15. IOTC, "Report of the Seventh Session of the IOTC Working Party on Tropical Tunas," *IOTC 7th Working Party for Tropical Tuna*, pp. 1-48 (2005).
16. Johnson, R. A., and Wichern D. W., *Applied Multivariate Statistical Analysis*. Prentice Hall, Englewood Cliffs, NJ, 607pp (1988).
17. Kaymaram, F., "The length-frequency analysis of yellowfin tuna in the Oman Sea," *IOTC Proceedings*, Vol. 1, pp. 216-218 (1998).
18. Kumari, B., Raman, M., Narain, A., and Sivaprakasam, T. E., "Location of tuna resources in Indian waters using NOAA AVHRR data," *International Journal of Remote Sensing*, Vol. 14, pp. 3305-3309 (1993).
19. Lee, M. A., Hsiao, C. H., and Liao, C. H., *The squid fishery oceanography in the NE waters of Taiwan - the fishing activity in relation to the oceanic features*. The Proceedings of International Conferences on the tropical & subtropical Fisheries. National Taiwan Ocean University, Taiwan, 20pp (2002).
20. Lee, M. A., Chang, Y., Sakaida, F., and Kawamura, H., "Validation of satellite-derived sea surface temperatures for waters around Taiwan." *Terrestrial, Atmospheric and Oceanic Sciences*, Vol. 16, No. 5, pp. 1189-1204 (2005a).
21. Lee, M. A., Yeah C. D., Cheng C. H., Chan, J. W., and Lee, K. T., "Empirical orthogonal function analysis of AVHRR sea surface temperature pattern in Taiwan Strait," *Journal of Marine Science and Technology*, Vol. 11, pp. 1-7 (2003).
22. Lee, P. F., Chen, I. C., and Tseng, W. N., *Distribution patterns of three dominant tuna species in the Indian Ocean*. 19th Intern. ERSI Users Conf., San Diego, CA, 10pp (1999).
23. Lee, Y. C., Nishida, T., and Mohri, M., "Separation of the Taiwanese regular and deep tuna longliners in the Indian Ocean using bigeye tuna catch ratios," *Fisheries Science*, Vol. 71, pp. 1256-1263 (2005b).
24. Lehodey, P., Andre, J.-M., Bertignac, M. *et al*., "Predicting skipjack tuna forage distributions in the equatorial Pacific using a coupled dynamical bio-geochemical model," *Fisheries Oceanography*, Vol. 7, pp. 317-325 (1998).
25. Li, X., Pichel W., Clemente-Colón P., Krasnopolsky, V., and Sapper, J., "Validation of coastal sea and lake surface temperature measurements derived from NOAA/AVHRR data," *International Journal of Remote Sensing*, Vol. 22, pp. 1285-1303 (2001).
26. Luis, A. J., and Pandey, P. C., "Characteristics of atmospheric divergence and convergence in the Indian Ocean inferred from scatterometer winds," *Remote Sensing of Environment*, Vol. 97, pp. 231-237 (2005).
27. Madhupratap, M., Kumar, S. P., Bhattathiri, P. M. A., Raghukumar, S., Nair, K. K. C., and Ramaiah, N., "Mechanism of the biological response to winter cooling in the northeastern Arabian Sea," *Letters to Nature*, Vol. 384, pp. 549-552 (1996).
28. Maunder, M. N., Sibert J. R., Fonteneau, A., Hampton, J., Kleiber, P., and Harley, S. J., "Interpreting catch per unit effort data to assess the status of individual stocks and communities," *ICES Journal of Marine Science: Journal du Conseil*, Vol. 63(8), pp. 1373-1385 (2006).
29. Miyake, M. P., Miyabe, N, and Nakano, H., "Historical trends of tuna catches in the world," *FAO Fisheries Technical Papers*, Vol. 467, pp. 1-74 (2004).
30. Marsac, F., "Climate and oceanographic indices appraising the environmental fluctuations in the Indian Ocean," *IOTC Proceedings*, Vol. 4, pp. 293-301 (2001).
31. Mohri, M., and Nishida, T., "Consideration on distribution of adult yellowfin tuna (*Thunnus albacares*) in the Indian Ocean based on Japanese tuna longline fisheries and survey information," *Journal of National Fisheries University*, Vol. 49, No. 1, pp. 1-11 (2000).
32. Nishida T., and Chen, D. G., "Incorporating spatial autocorrelation into the general linear model with an application to the yellowfin tuna (*Thunnus albacares*) longline CPUE data," *Fisheries Research*, Vol. 70, pp. 265-274 (2004).
33. Nishida T., Matsuura, H., Shiba, Y., Tanaka, M., Mohri, M., and Chang, S.-K., "Did ecological anomalies cause 1993 and 2003-2004 high catches of yellowfin tuna (*Thunnus albacares*) in the western Indian Ocean?" *IOTC 7th Working Party Tropical Tuna*, Vol. 27, pp. 24-41 (2005).
34. Nishida, T., Mohri, M., Itoh, K., and Nakagome, J., "Study of bathymetry effects on the nominal hooking rates of yellowfin tuna (*Thunnus albacares*) and bigeye tuna (*Thunnus obesus*) exploited by the Japanese tuna longline fisheries in the Indian Ocean," *IOTC Proceedings*, Vol. 4, pp. 191-206 (2005).
35. Nishida, T., and Shono, H., "Stock assessment of yellowfin tuna (Thunnus albacares) resources in the Indian Ocean by the age structured production model (ASPM) analyses," *IOTC Proceedings*, Vol. 5, pp. 248-273 (2002).
36. Ortega-García, S., and Lluch-Cota, S. E., *Distribución de la abundancia de atún y su relación con la concentración de pigmentos fotosintéticos derivados de satélite en aguas al sur de México*. Investigaciones Geográficas Boletín. Num. Especial 4. Instit. Geog. UNAM, Mexico (1996).
37. Pikitch, E. K., Santora, C., Babcock, E. A., Bakun, A. Bonfil, R., Conover, D. O., Dayton, P., Doukakis, P., Fluharty, D., Heneman, B., Houde, E. D., Link, J., Livingston, P. A., Mangel, M., McAllister, M.K. Pope, J., and Sainsbury, K.J., "Ecosystem-based fishery management," *Science*, Vol. 305, No. 5682, pp. 346-347 (2004).
38. Qasim, S. Z., "Oceanography of the northern Arabian Sea," *Deep Sea Research*, Vol. 29, No. 9a, pp. 1041-1068 (1982).
39. Rixen, T., Haake, B., Ittekkot, V., Guptha, M.V.S., Nair, R.R., and Schlussel, P., "Coupling between SW monsoon-related surface and deep ocean processes as discerned from continuous particle flux measurements and correlated satellite data," *Journal of geophysical research*, Vol. 101, pp. 28569-28582 (1996).
40. Robinson, M. K., Bauer, R. A., and Schroeder, E. H., *Atlas of the North Pacific Ocean monthly mean temperatures and mean salinities of the surface layer*. Naval Oceanographic Office, Dept. Navy, Washington, D.C., 19 pp (1976).
41. Singh, A., and Harrison, A., "Standardized principal components," *In-*

ternational Journal of Remote Sensing, Vol.6, 883-896 (1985).
42. Stequert, B. J. P., and Dean, J. M., "Age and growth of yellowfin tuna, Thunnus albacares, from the western Indian Ocean, based on otolith microstructure," *Fishery Bulletin*, Vol. 94, pp. 124-134 (1996).
43. Stretta, J.M., "Forecasting models for tuna fishery with aeroespatial remote sensing," *International Journal of Remote Sensing*, Vol. 12, No. 4, pp. 771-779 (1991).
44. Sund, P. N., Blackburn, M., and Willians, F., "Tunas and their environment in the Pacific Ocean: a review," *Oceanography and Marine Biology: an Annual Review*, Vol. 19, pp. 443-512 (1981).
45. Suzuki, Z., Tomlinson, P. K., and Honma, M., "Population structure of Pacific yellowfin tuna," *Inter-American Tropical Tuna Commission Bulletin*, Vol. 17, No. 5, pp 273-441 (1978).
46. Tang D. L., Kawamura, H., and Luis A. J., "Short-term variability of phytoplankton blooms associated with a cold eddy in the northwestern Arabian Sea," *Remote Sensing of Environment*, Vol. 81, pp. 28-89 (2002).
47. Tsai, C. F., and Chai, A. L., "Short-term forecasting of the striped bass (Morone saxatilis) commercial harvest in the Maryland portion of Chesapeake Bay," *Fisheries Research*, Vol. 15, pp. 67-82 (1992).
48. Wang, S. P., Chang, S. K., and Shono, H., "Standardization of CPUE for yellow-fin tuna catch by Taiwanses longline fishery in the Indian Ocean using generalized linear model," *IOTC Proceedings*, Vol. 8, pp. 14-23 (2005).
49. Wyrtki, K., *Physical oceanography of the Indian Ocean*. In "The Biology of the Indian Ocean." (B. Zeitschel, and Gerlach, S. A. eds.) Spring-Verlag, New York, pp. 18-36 (1973).
50. Yeh, Y. M., and Chang S. T., *CPUE Standardizations for Yellowfin Tuna Caught by Taiwanese Longline Fishery in the Indian Ocean Using Generalized Liner Model and Generalized Linear Mixed Model*. IOTC Working Party on Tropical Tuna, Kenya, 11pp (2009).
51. Yu, L., "Variability of the depth of the 20°C isotherm along 6°N in the Bay of Bengal: its response to remote and local forcing and its relation to satellite SSH variability," *Deep Sea Research Part II*, Vol. 50, pp. 2285-2304 (2003).
52. Zagaglia, C. R., Lorenzzetti, J. A., and Stech, J. L., "Remote sensing data and longline catches of yellowfin tuna (Thunnus albacares) in the equatorial Atlantic," *Remote Sensing of Environment*, Vol. 93, pp. 267-281 (2004).